Hindawi
Journal of Spectroscopy
Volume 2024, Article ID 5524783, 6 pages
https://doi.org/10.1155/2024/5524783

Research Article

Raman Spectra of PbTe- and GeTe-Based Monocrystalline Epitaxial Layers

N. Romcevic,[1] B. Hadzic,[1] P. Dziawa,[2] T. Story,[2,3] W. D. Dobrowolski,[2] and M. Romcevic[1]

[1]*Institute of Physics Belgrade, University of Belgrade, Pregrevica 118, Belgrade 11080, Serbia*
[2]*Institute of Physics, Polish Academy of Sciences, Aleja Lotnikow 32/46, Warsaw 02668, Poland*
[3]*International Research Centre MagTop, Institute of Physics, Polish Academy of Sciences, Aleja Lotnikow 32/46, Warsaw 02668, Poland*

Correspondence should be addressed to N. Romcevic; romcevi@ipb.ac.rs

Received 18 July 2023; Revised 26 February 2024; Accepted 5 March 2024; Published 11 March 2024

Academic Editor: Arnaud Cuisset

Lead telluride and germanium telluride are well-known IV-VI semiconductors, which is now the focus of research due to the perspective of application as thermoelectrics for midrange temperatures. Solid solutions and heterostructures on this basis, obtained by molecular beam epitaxy, are a promising direction for the development of these materials. In this paper, we have focused on the Raman spectra excited by the 514.5 nm laser line (out of resonance) of PbTe, GeTe, (Pb, Ge)Te, and (Pb, Ge, Eu)Te layers grown on BaF_2 (111) monocrystalline substrates. The obtained phonon properties are related to the properties of the corresponding bulk materials or can be explained by a model that takes into account the difference in the masses of the constituent elements only, as is the case with the local mode of Ge in PbTe (registered at about 181 cm^{-1}). Multiphonon processes registered for this phonon are a consequence of the change in the electronic structure of PbTe and electron-phonon interaction. An improvement in the quality of thin films due to doping with Eu ions was also registered.

1. Introduction

Lead telluride and germanium telluride are well-known IV-VI semiconductors [1]. They found their place in a large number of electronic devices and sensors, such as rewritable optical memory (CD, DVD) and electronic nonvolatile memory (NVM) technology [2, 3]. Recently, these materials are again in the focus of research due to the perspective of application as thermoelectrics for midrange temperatures (600–800 K) [4]. Very recent renewal of interest to (Pb, Ge)Te thin layers deposited on BaF_2 (111) substrates is related to their function as a novel ferroelectric Rashba semiconductor [5]. GeTe is a IV–VI narrow-gap semiconductor that, upon illumination or passing current, can transform between amorphous (resistive) and crystalline (metallic) states. Crystalline germanium telluride exists at room temperature in α (rhombohedral R3m) structure and at high temperatures in β (rocksalt-type phase—face centred cubic $Fm\bar{3}m$) at above 700 K [6]. PbTe has the cubic NaCl structure, where Pb and Te atoms form the cation and the anion sublattices. Properties of PbTe that depend on the dopants, such as an energy gap of 0.32 eV and the ability to be either n- or p-type, allowing it to be used for power generation applications. More recently, efforts have been made to improve the thermoelectric properties of PbTe by nanostructuring [4]. PbTe-based nanostructures have very favorable thermal and charge-transport properties. However, despite the promising results of new nanostructures based on PbTe, alloying in solid solution remains an active area of research [7].

Laboratory demonstrations showed highly efficient thermoelectric conversion parameters in mixed composite material (Pb, Ge)Te—Bi_2Te_3 [8]. Introduction of Eu in (Pb, Ge)Te is expected to open the band gap with a high rate of about 30 meV/at.% Eu, thus providing a way to tune the optimal operation temperature of thermoelectric converters.

Importantly, good thermoelectric materials must possess a very low thermal conductivity of the order of (1-2) W/mK. The engineering of thermal properties proved very successful in improving thermoelectric materials. However, this approach requires a detailed knowledge of phonon energies in binary, ternary, and quaternary IV-VI semiconductor alloys.

In this paper, we focused on the Raman spectra of PbTe, GeTe, (Pb, Ge)Te, and (Pb, Ge, Eu)Te layers that were grown on BaF_2 (111) monocrystalline substrates by the molecular beam epitaxy (MBE) technique. Our goal is to determine the phonon properties of this type of material in the form of thin films and provide guidelines for further synthesis that can lead to application as thermoelectrics.

2. Materials and Methods

PbTe, GeTe, (Pb, Ge)Te, and (Pb, Ge, Eu)Te layers on BaF_2 (111) monocrystalline substrates were grown by the molecular beam epitaxy (MBE) technique. Effusion cells with PbTe, GeTe, Eu, and Te solid sources were used, and the obtained layers were about 1 μm thick. Many growing processes were performed to obtain high crystalline-quality epitaxial heterostructures. Different samples with one or more layers (buffer layer at about 20–200 nm thick each) deposited on the BaF_2 (111) surface were produced. The layer growth was monitored in situ using the reflection high-energy electron diffraction (RHEED) technique. Typical RHEED diffraction observed during (Pb, Ge, Eu)Te deposition on BaF_2 presented in Figure 1(a) reveals the layer-by-layer 2D epitaxial growth regime. For composition determination of both Ge and Eu contents, we used XRD data and known Vegard law as well energy-dispersive X-ray fluorescence EDXF method. The content of Eu as well as the charge (2+) and spin state ($S = 7/2$) of Eu ions in (Pb, Ge, Eu)Te was verified by electron paramagnetic resonance experiments also.

In Figures 1(b)–1(d), we present representative XRD spectra for each group of films we analyzed. From this analysis, one draws the conclusion that all the samples where homogeneous, high quality crystalline layers. More details about obtaining this thin film type by the MBE method can be found in [9].

The micro-Raman spectra were taken in the backscattering configuration and analyzed by Jobin Yvon T64000 spectrometer, equipped with a nitrogen-cooled charge-coupled device detector. As an excitation source, we used the 514.5 nm (2.41 eV) line of an Ar-ion laser. A microscope lens with a magnification of 100x was used to focus the laser beam. The spectrum was recorded with a laser power density of 1.5 mW/μm^2 on the sample and the measurement time of 5 s, which did not cause structural changes in the sample.

Figures 2 and 3 show the Raman spectra of different layers based on PbTe and GeTe on the BaF_2 substrate at room temperature. The spectra were measured in a wide range, but only the results up to 1100 cm^{-1} are shown because the spectra are flat afterwards, without any specifics. The penetration depth of the laser radiation is such that the characteristics of both the film and the buffer layer can be seen on the spectra.

3. Results

Raman spectra of PbTe and GeTe on a BaF_2 substrate (in the designation PbTe/BaF_2 and GeTe/BaF_2) and GeTe on a PbTe buffer layer and a BaF_2 substrate (GeTe/PbTe/BaF_2) are shown in Figure 2(a).

The modes at 126 and 143 cm^{-1} are registered in all spectra. In addition, for samples with GeTe as the upper layer, phonons at 93, 160, 220, and 265 cm^{-1} were also registered. The spectra of PbTe/GeTe/BaF_2 and $Pb_{0.745}Ge_{0.255}Te/BaF_2$ are presented in Figure 2(b). In the case of PbTe/GeTe/BaF_2, in addition to the phonons registered in Figure 2(a), a new structure can be seen at around 73 cm^{-1} and 181 cm^{-1} as well as its second, third, and fourth order Raman scattering. For both samples, the phonon at 93 cm^{-1} is missing. It is interesting to note that in the PbTe/GeTe/BaF_2 sample, each harmonic has a different shape, i.e., there was a change in the shape of the harmonics relative to the $Pb_{0.745}Ge_{0.255}Te/BaF_2$ sample.

The spectra of $Ge_{0.989}Eu_{0.011}Te/BaF_2$ and representative sample of the (Ge, Eu)Te/GeTe/BaF_2 type are shown in Figure 3(a).

The addition of Eu did not lead to changes in the spectra compared to Figure 2(a). The exception is the shift of the phonon at 93 cm^{-1}–87 cm^{-1}. The effect of adding Eu to the PbGeTe solid solution is shown in Figure 3(b). For the $Pb_{0.697}Ge_{0.259}Eu_{0.044}Te$/PbGeTe/$BaF_2$ sample, the spectrum has all the characteristics of the spectra from Figure 2. However, for samples $Pb_{0.94}Ge_{0.049}Eu_{0.011}Te/BaF_2$ and $Pb_{0.91}Ge_{0.046}Eu_{0.044}Te/BaF_2$, it is characteristic that the phonons at 93, 126, and 143 cm^{-1} gave one broad structure, which occupies the range from 80 to 160 cm^{-1}. In addition, in all cases, the harmonics for the 181 cm^{-1} phonon have the same shape as for the PbTe/GeTe/BaF_2 sample.

4. Discussion

The results can be explained as follows. PbTe has a cubic structure of the NaCl type ($Fm\bar{3}m$ space group symmetry) and no active Raman modes. Phonon at about 73 cm^{-1} (see Figure 2(b)) is the Brillouin zone edge mode because the phonon density of PbTe [10] has a maximum at these frequencies. This mode has already been observed in many PbTe-based alloys. PbTe at the top of the structure or in a large percentage in the alloy (see Figure 3(b)) does not allow the 93 cm^{-1} phonon GeTe to be seen. The broad but weak structure at about 100 cm^{-1} in Figure 3(b) is the sum of phonons from GeTe at about 93 cm^{-1} and phonons from PbTe at about 104 cm^{-1}. In both cases, they phonons were registered for violating the selection rules. Regarding phonons at 126 and 143 cm^{-1}, registered in Figure 2(a) for PbTe/BaF_2, but also on most other spectra from the literature [11, 12], it is known that these modes originate from the TeO_2, which is always formed on the sample surface. These modes can weaken if the single crystal sample is polished immediately before the measurement. Also, TeO_2 is much thinner than the penetration depth of the laser light, so it does not affect the accuracy of the Raman spectrum. Of course, polishing is out of the question for samples obtained by MBE. However, this is not the main topic of this paper.

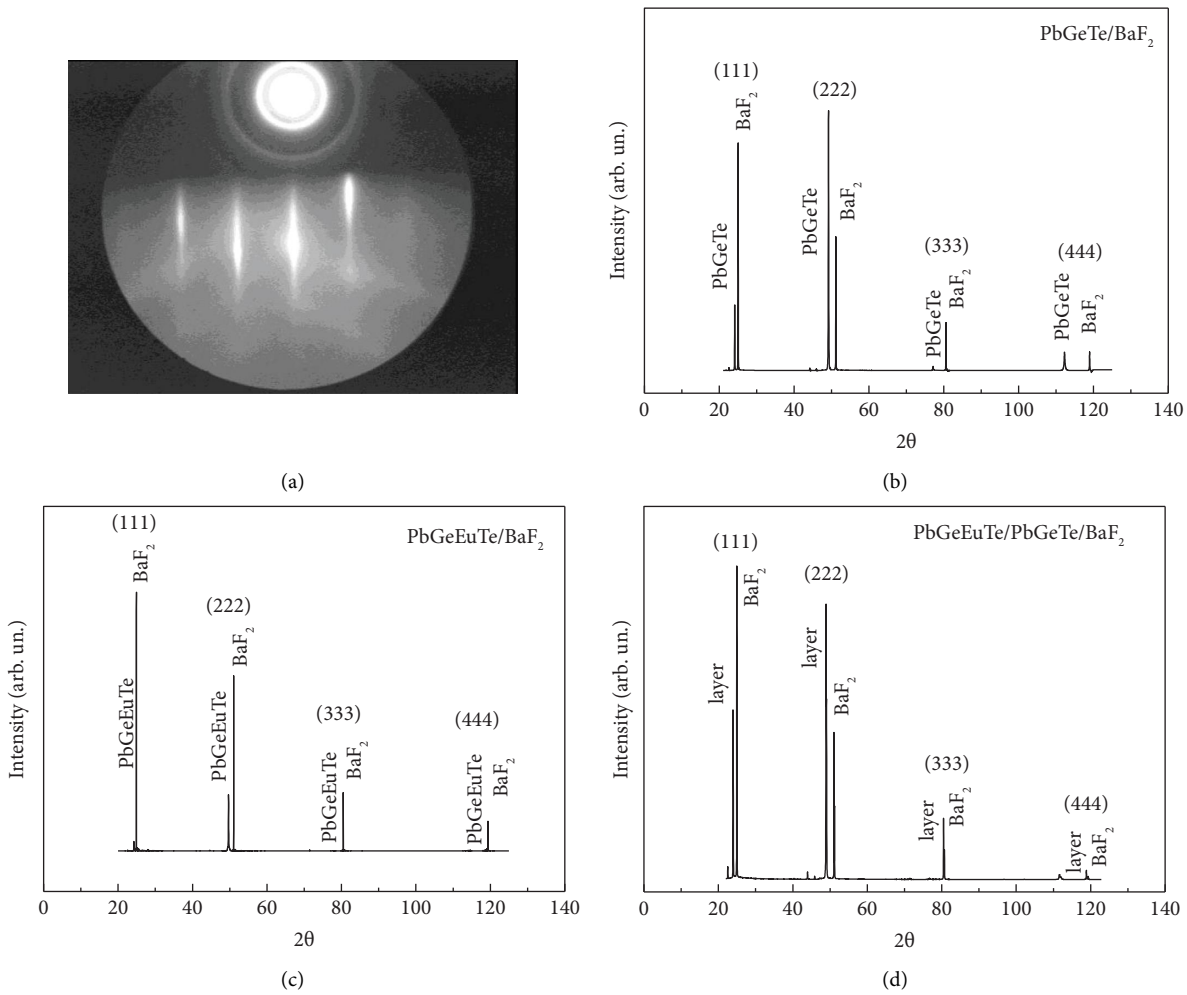

Figure 1: (a) RHEED diffraction observed during (Pb, Ge, Eu)Te deposition on BaF_2. XRD spectrum for (Pb, Ge)Te/BaF_2 (b), (Pb, Ge, Eu) Te/BaF_2 (c), and (Pb, Ge, Eu)Te/(Pb, Ge)Te/BaF_2 (d).

In the case of GeTe spectra, the situation is somewhat more complicated. In the high temperature cubic phase of GeTe, Raman scattering by optical phonons is forbidden, as in the case of PbTe. However, in the case of the room temperature phase of the rhombohedral structure with cation-anion sublattice shift (ferroelectric distortion), scattering is allowed due to the absence of inverse symmetry. There are several works on this topic [13–15]. Based on this, it can be concluded that the mode at 93 cm^{-1} originates from the distorted octahedrally coordinated Ge atoms. Also, the mode at about 160 cm^{-1} corresponds to the vibrations of Ge atoms on defective octahedral sites [16]. The weak structures around 220 cm^{-1} and 265 cm^{-1} can be related to Ge vibrations in the $GeTe_{4\text{-}n}Ge_n$ environment [14, 15] or the sum of TeO_2 vibrations, which are now seen as the second harmonic.

We labeled the structure at $\omega_0 = 181\ cm^{-1}$ from Figure 3 as a local Ge mode. It is known that if the semiconductor is doped with impurities that take the place of a heavier atom and are lighter than it; in our case, Ge takes the place of Pb in PbTe and then two new modes appear. These are the local mode, which appears above the optical band, and the gap mode, located between the acoustic and optical bands of the host material [17]. In the case of PbTe, that gap does not exist, so the gap mode does not appear.

The impurity mode can appear due to the electron-phonon interaction [18]. Still, most often, it occurs due to the difference in the masses of the original ion and the impurity that comes in its place, known as the isotope like or mass effect [19]. In our case, lattice ions are replaced with lighter ones, and we approximate no change in the force constants.

If only the mass effect is taken into account, the position of the local mode can be estimated in the simplest way, which is described in detail in [20].

$$\frac{\omega_o}{\omega_{LO\,PbTe}} = \sqrt{\frac{m_{\mathrm{Pb}}}{m_{\mathrm{Ge}}}}, \tag{1}$$

In this way, the value for $\omega_0 = 175.7\ cm^{-1}$ was determined. That value is in very good agreement with the experimental values from Figures 2(b) and 3(b).

Higher harmonics were registered for the local mode of Ge in PbTe (Figures. 2(b) and 3(b)). For all samples from

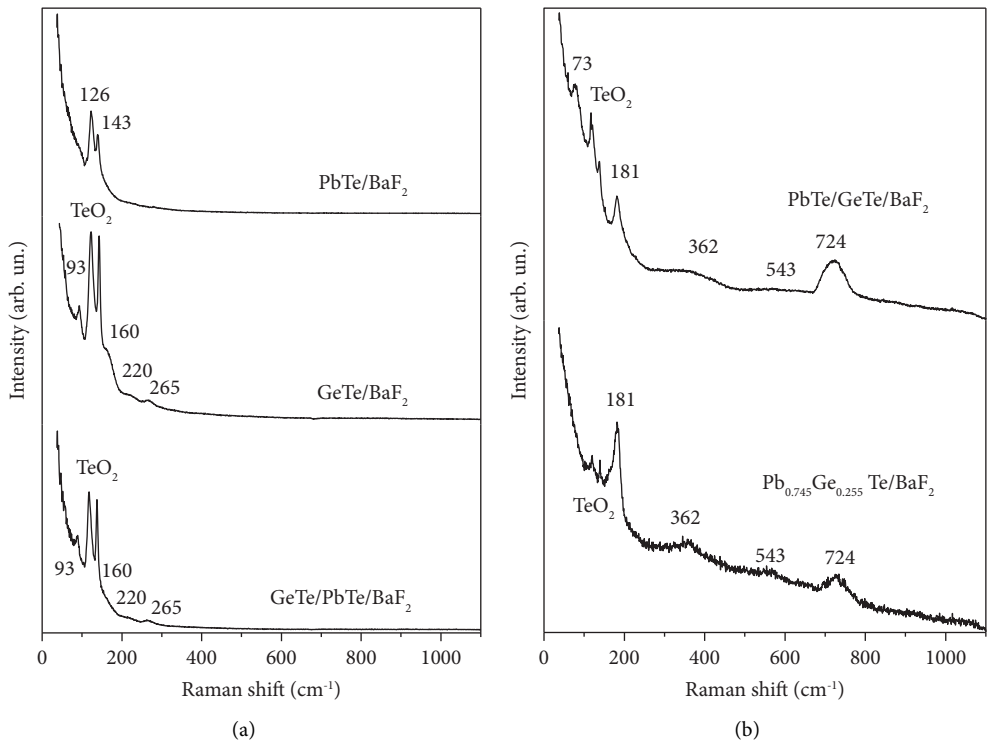

Figure 2: (a) Raman spectra of $PbTe/BaF_2$, $GeTe/BaF_2$, and $GeTe/PbTe/BaF_2$ and (b) Raman spectra of $PbTe/GeTe/BaF_2$ and $Pb_{0.745}Ge_{0.255}Te/BaF_2$.

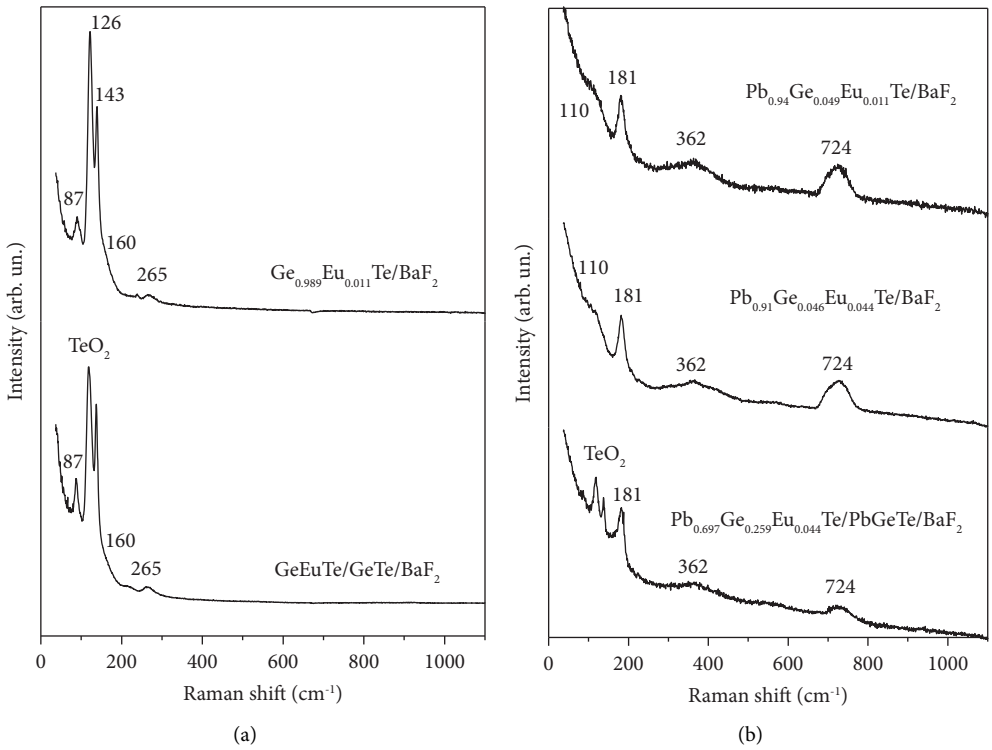

Figure 3: (a) Raman spectra of $Ge_{0.989}Eu_{0.011}Te/BaF_2$ and (Ge, Eu)Te/GeTe/BaF_2 and (b) Raman spectra of $Pb_{0.94}Ge_{0.049}Eu_{0.011}Te/BaF_2$, $Pb_{0.91}Ge_{0.046}Eu_{0.044}Te/BaF_2$, and $Pb_{0.697}Ge_{0.259}Eu_{0.044}Te/(Pb,Ge)Te/BaF_2$.

Figures 2(b) and 3(b), we note that the third harmonic is significantly weaker in intensity than the second and fourth. For the sample $Pb_{0.745}Ge_{0.255}Te/BaF_2$, all harmonics have only phononic character, i.e., there are no features related to the electron-phonon interaction, such as broadening relative to the natural form, change of position regarding the basic multiplied value, and formation of a new structure near the multiphonon. However, the fourth harmonic in the $PbTe/GeTe/BaF_2$ sample has all these characteristics.

The explanation for this situation can be as follows: during the growth of this heterostructure by the MBE method, there is no sharp transition from the GeTe layer to the upper PbTe layer, but rather the formation of a PbTe-GeTe transition layer. This spatial inhomogeneity has nanometer dimensions and plays a very active role. Because of its dimensions, it causes changes in the electronic structure, which can lead to electron-phonon interaction, as in our case. One of the consequences of the electron-phonon interaction on the Raman spectra is the change in the shape of the harmonic (in our case, the fourth) [21]. The energy of this harmonic is close to the energy of the electronic transition, so the conditions for interaction between them have been created. The energy of the fourth harmonic is about 100 meV. In the energy spectrum of PbTe, several transitions exist in this energy range [1]. Therefore, the conditions for electron-phonon interaction were created in this way. This effect is desired when designing new thermoelectrics.

The same effect with the fourth harmonic can be seen in the samples from Figure 3(b). However, the reason for registering the electron-phonon interaction is the addition of Eu ions. These ions do not create new levels or resonance states [9]. Still, they change the electronic spectrum of the basic material, so similarly, the energy of the fourth phonon and electronic transitions in the PbTe alloy are brought closer together. As a result, the shape of the fourth harmonic changes again.

Further research should focus on the thermoelectric properties of these heterostructures and the search for the optimal level of Eu doping, which will be the subject of our future work.

5. Conclusion

In this paper, we have focused on the Raman spectra of PbTe, GeTe, (Pb, Ge)Te, and (Pb, Ge, Eu)Te layers grown on BaF_2 (111) monocrystalline substrates. Phonon features originating from the bulk material and a local mode of Ge in PbTe at about 181 cm^{-1} were registered. The position of this local mode can be explained by a model that only considers the difference in the masses of the constituent elements. Multiphonon processes registered for this phonon are a consequence of the change in the electronic structure of PbTe. The shape of the fourth harmonic of the Ge local mode in PbTe in the $PbTe/GeTe/BaF_2$ heterostructure and (Pb, Ge, Eu)Te-based films is a consequence of the influence of electron-phonon interaction on the intensity of Raman scattering lines.

Data Availability

The data used to support the findings of this study are available from the corresponding author upon reasonable request.

Conflicts of Interest

The authors declare they have no conflicts of interest.

Authors' Contributions

N. Romcevic contributed to conceptualization, methodology, formal analysis, and original draft preparation; B. Hadzic, P. Dziawa, T. Story, and W. D. Dobrowolski contributed to investigation and formal analysis; and M. Romcevic contributed to investigation, formal analysis, and reviewing and editing. All the authors have read and agreed to the published version of the manuscript.

Acknowledgments

This work was realized under the Agreement of Scientific Collaboration between Polish Academy of Science and Serbian Academy of Sciences and Arts. The authors thank V. Domukhovski for help with XRD measurements. This research was supported by the Science Fund of the Republic of Serbia, Grant no. 7504386, Nano object in own matrix–Self composite–NOOM-SeC. T.S. The authors also acknowledge the support by the Foundation for Polish Science through the International Research Agendas cofinanced by EU within Smart Growth Operational Programme.

References

[1] Y. I. Ravich, B. A. Efimova, and I. A. Smirnov, *Semiconducting Lead Chalcogenides*, Plenum, New York, NY, USA, 1970.

[2] F. Ren, E. D. Case, J. R. Sootsman et al., "The high-temperature elastic moduli of polycrystalline PbTe measured by resonant ultrasound spectroscopy," *Acta Materialia*, vol. 56, no. 20, pp. 5954–5963, 2008.

[3] Y. Gelbstein, Z. Dashevsky, and M. P. Dariel, "The search for mechanically stable PbTe based thermoelectric materials," *Journal of Applied Physics*, vol. 104, no. 3, Article ID 033702, 2008.

[4] J.-D. Musah, A. M. Ilyas, S. Venkatesh et al., "Isovalent substitution in metal chalcogenide materials for improving thermoelectric power generation – a critical review," *Nano Research Energy*, vol. 1, no. 3, Article ID e9120034, 2022.

[5] G. Krizman, T. Zakusylo, L. Sajeev et al., "A novel ferroelectric Rashba semiconductor," *Advanced Materials*, vol. 23, Article ID e2310278, 2023.

[6] W. D. Johnston and D. E. Sestrich, "The MnTe-GeTe phase diagram," *Journal of Inorganic and Nuclear Chemistry*, vol. 19, no. 3–4, pp. 229–236, 1961.

[7] P. F. P. Poudeu, J. D'Angelo, H. Kong et al., "Nanostructures versus solid solutions: low lattice thermal conductivity and enhanced thermoelectric figure of merit in $Pb_{9.6}Sb_{0.2}Te_{10-x}Se_x$ bulk materials," *Journal of the American Chemical Society*, vol. 128, no. 44, pp. 14347–14355, 2006.

[8] Y. Gelbstein, B. Dado, O. Ben-Yehuda, Y. Sadia, Z. Dashevsky, and M. P. Dariel, "Highly efficient Ge-rich $Ge_xPb_{1-x}Te$ thermoelectric alloys," *Journal of Electronic Materials*, vol. 39, no. 9, pp. 2049–2052, 2009.

[9] T. Radzynski, A. Lusakowski, K. Swiatek, and T. Story, "The influence of microscopic disorder on electron paramagnetic resonance spectra of Eu^{2+} ions in $Pb_{1-x}Ge_xTe$," *Journal of Physics: Condensed Matter*, vol. 21, no. 40, Article ID 405802, 2009.

[10] W. Cochran, R. A. Cowley, G. Dolling, and M. M. Elcombe, "The crystal dynamics of lead telluride," *Proceedings of the Royal Society*, vol. 293, p. A433, 1966.

[11] J. H. Cape, L. G. Hale, and W. Tennant, "Raman scattering studies of monolayer-thickness oxide and tellurium films on PbSnTe," *Surface Science*, vol. 62, no. 2, pp. 639–646, 1977.

[12] A. S. Pine and G. Dresselhaus, "Raman spectra and lattice dynamics of tellurium," *Physical Review B*, vol. 4, no. 2, pp. 356–371, 1971.

[13] G. Kalra and S. Murugavel, "The role of atomic vacancies on phonon confinement in α-GeTe," *AIP Advances*, vol. 5, no. 4, Article ID 047127, 2015.

[14] M. Upadhyay, S. Murugavel, M. Anbarasu, and T. R. Ravindran, "Structural study on amorphous and crystalline state of phase change material," *Journal of Applied Physics*, vol. 110, no. 8, Article ID 083711, 2011.

[15] R. Mazzarello, S. Caravati, S. Angioletti-Uberti, M. Bernasconi, and M. Parrinello, "Signature of tetrahedral Ge in the Raman spectrum of amorphous phase-change materials," *Physical Review Letters*, vol. 104, no. 8, Article ID 085503, 2010.

[16] K. S. Andrikopoulos, S. N. Yannopoulos, G. A. Voyiatzis, A. V. Kolobov, M. Ribes, and J. Tominaga, "Raman scattering study of the a-GeTe structure and possible mechanism for the amorphous to crystal transition," *Journal of Physics: Condensed Matter*, vol. 18, no. 3, pp. 965–979, 2006.

[17] A. J. Sievers and K. D. Moller, *Far Infrared Spectroscopy*, W. B. Rothschild, Ed., Wiley, New York, NY, USA, 1971.

[18] A. A. Gogolin and E. I. Rashba, "Mechanism of strong resonant 1LO Raman scattering," *Solid State Communications*, vol. 19, no. 12, pp. 1177–1179, 1976.

[19] N. Romcevic, J. Trajic, T. A. Kuznetsova, M. Romcevic, B. Hadzic, and D. R. Khokhlov, "Far-infrared study of impurity local modes in Ni-doped PbTe," *Journal of Alloys and Compounds*, vol. 442, no. 1-2, pp. 324–327, 2007.

[20] J. Mitric, U. Ralevic, M. Mitric et al., "Isotope-like effect in YVO_4:Eu^{3+} nanopowders: Raman spectroscopy," *Journal of Raman Spectroscopy*, vol. 50, no. 6, pp. 802–808, 2019.

[21] M. Gilic, N. Romcevic, M. Romcevic et al., "Optical properties of CdTe/ZnTe self-assembled quantum dots: Raman and photoluminescence spectroscopy," *Journal of Alloys and Compounds*, vol. 579, pp. 330–335, 2013.